

Pushing the Memory Bandwidth Wall with CXL-enabled Idle I/O Bandwidth Harvesting

Divya Kiran Kadiyala

School of Electrical and Computer Engineering
Georgia Institute of Technology
Atlanta, Georgia, USA

Email: dkadiyala3@gatech.edu

Alexandros Daglis

School of Computer Science
Georgia Institute of Technology
Atlanta, Georgia, USA

Email: alexandros.daglis@cc.gatech.edu

Abstract—The continual increase of cores on server-grade CPUs raises demands on memory systems, which are constrained by limited off-chip pin and data transfer rate scalability. As a result, high-end processors typically feature lower memory bandwidth per core, at the detriment of memory-intensive workloads. We propose alleviating this challenge by improving the utility of the CPU’s limited pins. In a typical CPU design process, the available pins are apportioned between memory and I/O traffic, each accounting for about half of the total off-chip bandwidth availability. Consequently, unless both memory and I/O are simultaneously highly utilized, such fragmentation leads to underutilization of the valuable off-chip bandwidth resources. An ideal architecture would offer *I/O and memory bandwidth fungibility*, allowing use of the aggregate off-chip bandwidth in the form required by each workload.

In this work, we introduce SURGE, a software-supported architectural technique that boosts memory bandwidth availability by salvaging idle I/O bandwidth resources. SURGE leverages the capability of versatile interconnect technologies like CXL to dynamically multiplex memory and I/O traffic over the same processor interface. We demonstrate that SURGE-enhanced architectures can accelerate memory-intensive workloads on bandwidth-constrained servers by up to 1.3 \times .

I. INTRODUCTION

Modern server-grade CPUs with growing core counts are appealing to datacenter operators as enablers of improved workload consolidation and, by extension, total cost of ownership. However, challenges in scaling memory bandwidth commensurately with cores result in reduced bandwidth-per-core availability for CPUs at the higher end of core count. Therefore, such manycore CPUs are more vulnerable to the well-known memory bandwidth wall challenge [49].

The memory wall arises from limited off-chip bandwidth: CPU pin density has only doubled every six years [43], while data transfer rate scaling faces power and signal integrity limits [10], [30]. Because of this pin scarcity, statically partitioning off-chip bandwidth between memory and I/O at design time risks wasteful *bandwidth stranding*. For example, a workload may saturate memory bandwidth while leaving I/O bandwidth underused (or vice versa). In such cases, workloads become bandwidth-bottlenecked despite unused off-chip capacity. With the common 1:1 memory-to-I/O provisioning ratio, the fraction of stranded bandwidth can be substantial.

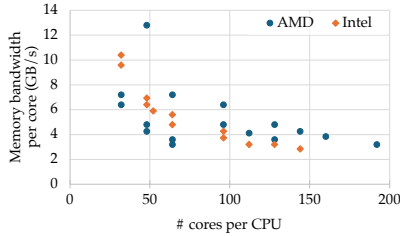
Eliminating stranding requires treating all off-chip bandwidth as interchangeable between memory and I/O. This

work targets one instance of that problem: relieving memory bandwidth pressure on modern manycore CPUs. Our key insight is that servers often leave much of their I/O bandwidth underutilized, which we propose to salvage for gains in efficiency (SURGE). For instance, PCIe-attached SSDs are often used only as boot volumes [5], [29], so they see little activity during normal operation. Similarly, many workloads generate little network traffic, leaving high-bandwidth NICs idle [51]. For example, Benson et al. report that (i) 70% of server network links use less than 1% of capacity [7], and (ii) the 95th-percentile utilization over 10 days is under 25% [8]. As a result, significant CPU bandwidth capacity designated for I/O at design time often remains unused across datacenter servers. SURGE dynamically converts this idle I/O bandwidth into extra memory bandwidth when needed.

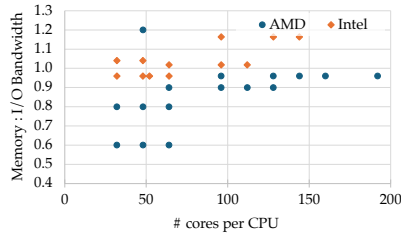
In this paper, we investigate the potential of integrating our proposed SURGE technique in server-grade systems. To maximize SURGE’s potential, our design encompasses hardware extensions to support dynamic I/O and memory traffic multiplexing on the same CPU off-chip interface, along with auxiliary software at the OS memory manager and cluster manager level. We identify the emerging Compute Express Link (CXL) interconnect [16] as a timely and fitting technology to support SURGE’s interface multiplexing requirement, and use it to evaluate two SURGE embodiments—SURGE Solo and SURGE Pod—that introduce different memory provisioning requirements with associated cost and utility implications.

Using SURGE to salvage memory bandwidth over an underutilized I/O link requires provisioning a memory device (“salvage memory”) connected via that multiplexed link. In SURGE Solo, salvage memory is directly connected to a single CPU. Whenever that CPU exhibits high I/O activity, salvage memory becomes unreachable, causing wasteful and costly *memory capacity stranding*. SURGE Pod alleviates this drawback by pooling salvage memory within small CPU groups. Our analysis shows SURGE Pod’s benefits for resource provisioning and performance.

We evaluate our proposed SURGE architecture using throughput workloads and online services with a range of I/O utilization scenarios. SURGE benefits memory-bound workloads, yielding speedups of up to 1.24 \times when the server’s I/O subsystem is idle and up to 1.2 \times even under high I/O



(a) Mem. bandwidth availability per core.



(b) Memory to I/O bandwidth availability.

Fig. 1: Bandwidth characteristics of modern manycore processors. SKUs sampled from the AMD EPYC and Intel Xeon server processor families.

activity. In summary, we make the following contributions:

- We propose idle I/O bandwidth salvaging to alleviate the memory wall for bandwidth-strapped manycore CPUs.
- We introduce SURGE, a novel software-assisted architectural mechanism that leverages opportunistic I/O bandwidth salvaging to boost memory bandwidth availability.
- We evaluate a CXL-based implementation of SURGE and analyze resource-provisioning tradeoffs introduced by two distinct architectural embodiments: Solo and Pod.
- We evaluate SURGE with diverse workloads and I/O activity levels, achieving speedups of up to 1.3×.

Paper outline: §II provides background on memory and I/O bandwidth allocation in modern CPUs, and introduces the opportunity for dynamic memory and I/O traffic multiplexing. §III presents SURGE, a design that effectively leverages the technique of idle I/O salvaging, and §IV details a SURGE implementation using CXL as the enabling interface. We detail our methodology in §V and evaluate SURGE in §VI. Finally, §VII discusses related work and §VIII concludes.

II. BACKGROUND

A. The Memory Bandwidth Wall

The memory bandwidth available per core has been decreasing in recent high-core-count processors, creating a significant performance bottleneck for bandwidth-hungry workloads. This trend arises from the architectural constraints of modern DDR-based memory systems. As core counts increase, memory bandwidth does not scale proportionally, primarily due to limitations in the number of memory channels that can be supported by a processor. Each DDR channel requires 288 physical pins (160+ on the processor side), which are limited by package size and signal integrity constraints [12]. Furthermore, while DDR generations increase data rates, signal integrity challenges and power concerns have slowed the improvement rate [30], [52].

Fig. 1a shows the per-core memory bandwidth availability of various recent high-end manycore CPUs, as a function of core count. Evidently, scaling bandwidth availability to keep up with core count is challenging. The resulting reduction in per-core bandwidth becomes especially problematic for bandwidth-intensive workloads. Fig. 2 presents the per-core bandwidth requirements of several workloads we use in our

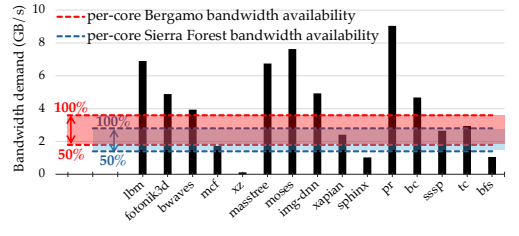


Fig. 2: Per-core memory bandwidth demands across evaluated workloads and ranges where two modern CPUs encounter queuing delays.

evaluation (details in §V). When compared against the per-core memory bandwidth available on processors with the highest core counts, such as Intel Sierra Forest (144 cores, 2.8 GB/s per core) and AMD Bergamo (128 cores, 3.6 GB/s per core), it is evident that many workloads approach or even exceed the bandwidth capacity available per core. Even when the nominal bandwidth availability is not exceeded, it is well known that memory contention affects memory access time, with considerable queuing delays kicking in beyond ~50% utilization [12], [18], [48]. As highlighted in Fig. 2, when deployed on those CPUs, the bandwidth demand of most of our evaluated workloads either exceeds bandwidth availability, or falls in the operational range of high contention.

This mismatch between workload demands and architectural supply reinforces the memory bandwidth wall as a limiting factor in the scalability and efficiency of modern manycore systems. In this paper, we focus on the subclass of processors at the high end of the core count spectrum to explore the implications of limited per-core memory bandwidth on workload performance and system design.

B. Processor Off-chip Bandwidth Allocation

A processor’s off-chip memory bandwidth availability is capped by the limited number of pins available per socket. Due to physical properties and mechanical constraints, pin density scalability is challenging and lags behind silicon scaling [43]. The absolute off-chip data movement rate a processor can achieve over its limited pins also depends on the signaling and protocol employed—for example, serial interfaces are considerably more pin-efficient than DDR [12].

The available pins (and, by extension, the off-chip bandwidth they supply) are typically statically partitioned at design time between memory and I/O interfaces (typically DDR and PCIe). Off-chip bandwidth is divided roughly equally between memory and I/O. Fig. 1b shows that the memory to I/O bandwidth division ratio ranges between 0.6 and 1.2 (0.94 on average) for the same set of server-grade CPUs shown in Fig. 1a. Such static division of off-chip bandwidth into two non-interchangeable resource groups prevents dynamic bandwidth allocation where it is most needed. For example, a processor handling a workload that uses all available memory bandwidth but no I/O bandwidth would encounter a perfor-

mance bottleneck, while leaving about half of its off-chip bandwidth resources (i.e., those reserved for I/O) idle.

C. Pin Multiplexing with Compute Express Link

Overcoming the limitation of static, design-time off-chip bandwidth allocation by dynamically reallocating provisioned I/O bandwidth to memory can help scale past the memory bandwidth wall. The first requirement for such an architecture is a unified protocol and interface that support seamless multiplexing of I/O and memory traffic.

Compute Express Link (CXL) [16] is an emerging interconnect that provides this capability. CXL is layered over the high-speed PCIe serial interface but replaces PCIe’s transport layer to extend functionality. It supports three protocols: CXL.io for conventional I/O devices, CXL.mem for disaggregated memory (enabling direct ld/st access to “Type 3” memory devices), and CXL.cache for coherent accelerator attachment, which is beyond the scope of this work. A single CXL interface supports all three protocols and can dynamically multiplex their traffic over the same physical link. We leverage this feature to improve off-chip bandwidth utilization and mitigate the memory wall.

Owing to its underlying serial interface, CXL is highly bandwidth efficient, delivering at least $4\times$ higher bandwidth per pin than DDR [12]. However, the several SerDes conversions required on the critical path considerably increase the latency to access a CXL-attached memory device. This latency penalty can range from 50 to over 100 ns depending on the system architecture and distance to the memory device [12], [24], establishing CXL-attached memory as a more likely secondary tier than a replacement for conventional DDR-attached memory. However, while such latency premium seems prohibitive compared to the raw DRAM access latency of ~ 50 ns, it is less so when considering the end-to-end memory access latency on a manycore CPU (e.g., 120 ns unloaded memory access time on a 128-core AMD Bergamo) and queuing delays due to contention on a highly utilized memory system, as we further analyze in §III-B2.

A second key differentiating CXL feature over DDR is that it is full-duplex—i.e., CXL can fully utilize its offered bandwidth in both directions simultaneously. In contrast, DDR provides unidirectional bandwidth for memory reads and writes. To illustrate, while a DDR5-4800 channel can move an *aggregate* of 38.4 GB/s read/write traffic, a CXL-3.* x8 channel can both receive (RX) *and* transmit (TX) at 32 GB/s simultaneously. This capability highlights the opportunity for directional multiplexing of a CXL interface. For example, a TX-heavy workload streaming data out to an I/O device leaves plenty of bandwidth availability on the RX path that could be leveraged to boost memory read bandwidth availability.

Building on these insights, we investigate a flexible bandwidth-boosting mechanism that opportunistically salvages idle I/O bandwidth to increase memory bandwidth availability for memory-bound systems. Our proposed architectural approach stands in contrast to the static design-time off-chip bandwidth partitioning in current systems, enabling improved utilization

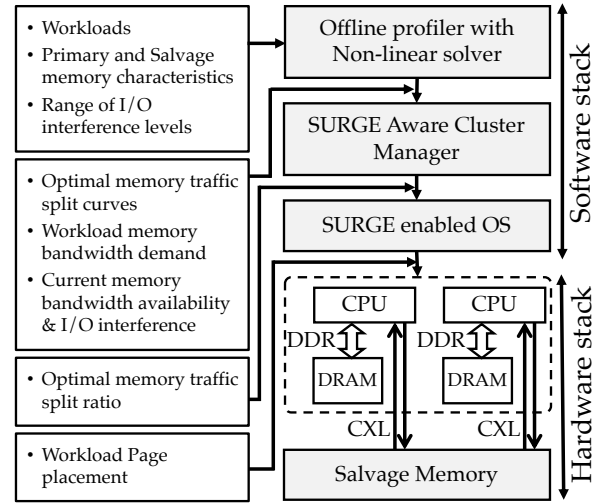


Fig. 3: SURGE hardware and software components.

of precious off-chip bandwidth resources on modern manycore processors that dynamically adapts to workload demand.

III. SURGE DESIGN

Allowing dynamic multiplexing of memory and I/O bandwidth resources mitigates the inefficiency of statically partitioning a processor’s off-chip bandwidth statically between memory and I/O at design time. We propose SURGE, an instance of such a multiplexing approach that targets memory-bound workloads. SURGE aims to boost memory bandwidth availability by dynamically salvaging idle I/O resources.

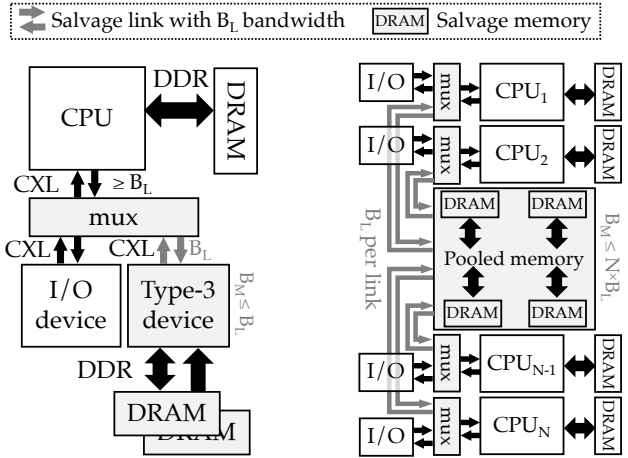
Fig. 3 shows SURGE’s high-level design. SURGE consists of architectural extensions along with software support to maximize the hardware technique’s utility. On the architectural front (§III-A), the processor must be provisioned with additional memory that can be accessed via I/O interfaces, which must also be configured to allow multiplexing of memory traffic. Maximizing the benefit derived from SURGE’s architectural extensions requires software support that drives deployment and configuration decisions (§III-B).

A. Architectural Support

We investigate two architectural design instances. The first, simpler one targets I/O bandwidth salvaging at the individual server level while the second extends the approach to cluster scale. We describe the two designs in §III-A1–§III-A2 and compare their resource efficiency in §III-A3.

SURGE is not intricately tied to any specific protocol or off-chip interface fabric; it only fundamentally requires the capability of dynamic I/O and memory traffic multiplexing. CXL represents a promising technology meeting that requirement, thus we focus on it to facilitate a quantitative narrative.

1) *SURGE Solo*: Fig. 4a shows the simplest form of SURGE, which targets individual servers. Consider a CXL-capable PCIe interface with an attached I/O device, such as a NIC. SURGE Solo bifurcates this interface: the primary link



(a) Solo SURGE. Sharing a CXL interface channel between an I/O device and a CXL Type 3 device as salvage memory.

(b) SURGE Pod. Sharing a CXL Type 3 multi-headed memory device as salvage memory across multiple servers.

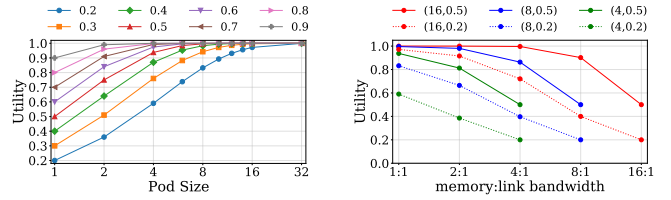
Fig. 4: Two SURGE architectural embodiments.

connects to the I/O device, while a secondary link connects to a memory device—in CXL terminology, a “Type 3” device. We refer to the added link and memory as *salvage link* and *salvage memory*, respectively. A simple arbiter performs the dynamic multiplexing of I/O and memory traffic, by directing each type of traffic to the respective device. We discuss its functionality in more detail in §IV-A.

The hardware extension’s key performance parameters are the latency overhead and bandwidth B_L of the salvage link, and the bandwidth $B_M \leq B_L$ of the salvage memory. The former two parameters are dictated by the used interface. For CXL, the B_L of a 16-lane PCIe 5 interface is 63 GB/s per direction, with a 50–100 ns latency overhead over direct DDR access [12]. B_M depends on the DDR memory channels provisioned on the Type 3 device. For example, a 16-lane CXL link can comfortably accommodate a DDR5-4800 channel’s 38.4 GB/s of bandwidth or a couple of DDR4-3200 channels.

2) *SURGE Pod*: SURGE Pod, shown in Fig. 4b, is an alternative design point leveraging the same fundamental technique of opportunistic idle I/O bandwidth salvaging, but the provisioned salvage memory is *pooled* across multiple servers that are logically grouped together in a *pod*, as in prior architectures proposed to mitigate memory capacity stranding [9], [24]. The pooled memory is a CXL Type 3 Multi-Headed Device, featuring multiple CXL ports to support direct connections to every server in the pod. In contrast to SURGE Solo, provisioning $B_M > B_L$ is plausible, as it allows multiple servers to use the salvage memory device simultaneously. §III-A3 elaborates on B_M provisioning considerations.

3) *Utility Comparison*: SURGE Solo and Pod represent different design points in resource provisioning and utility. Because salvage memory is accessible only via a single salvage link, high I/O activity on that link strands the memory—an undesirable and costly waste of resources. We define *utility*



(a) Utility for various P values, as a function of pod size. Pod size of 1 is SURGE Solo.

(b) Utility for various (pod size, P) combinations as a function of provisioned $B_M:B_L$ ratio.

Fig. 5: Salvage memory utility for SURGE as a function of pod size and P (probability of each individual salvage link having sufficient idle bandwidth to be salvaged by SURGE).

as the probability of using a salvage memory’s provisioned bandwidth, with stranding probability as its inverse. Designing a practical SURGE system thus requires balancing the cost of provisioned salvage memory against its expected utility. We use memory bandwidth as the primary metric, assuming it correlates directly with both memory capacity and cost.

A key drawback of SURGE Solo relative to Pod is its low utility: when a server’s I/O bandwidth is fully utilized, salvaging memory bandwidth is impossible, leaving the attached salvage memory stranded. In contrast, SURGE Pod’s pooling of salvage memory substantially reduces the probability of stranding, as Fig. 5a demonstrates. If the probability that a cluster’s server has sufficient idle I/O bandwidth to salvage is P , then the utility of SURGE Solo is P . For an N -server pod, utility increases to $1 - (1 - P)^N$. For example, with $P = 20\%$ and $N = 16$, utility rises from 20% to 97%.

SURGE Pod introduces the additional consideration of memory bandwidth provisioning, B_M . For an N -node pod with N salvage links of bandwidth B_L , B_M may range from B_L to $N \times B_L$, with utility also factoring into the decision. Fig. 5a assumed $B_M = B_L$. Fig. 5b plots utility for two pod sizes and two values of P as a function of B_M . On the x-axis, $X:1$ denotes $B_M = X \times B_L$. Utility declines more quickly with smaller pods and higher P . For example, a 16-node pod with $B_M = 4 \times B_L$ maintains over 80% utility even with $P = 20\%$. In general, sustaining high utility favors modest B_M provisioning.

While larger pods offer higher utility, they introduce two overheads: (i) greater interconnect complexity and cost, and (ii) higher latency to access remote memory, with prior work reporting 75–100 ns additional latency for groups of 8–16 servers [11], [24]. While a cost analysis is beyond the scope of this paper, Fig. 5’s utility results indicate a pod size sweet spot around 8, with diminishing returns beyond that. We focus on the potential of SURGE as an architectural technique.

B. Software Support

1) *Workload Placement by Cluster Manager*: SURGE’s premise is that there exists ample idle I/O bandwidth to be salvaged in order to boost memory bandwidth availability. Whether that condition is true depends on the workload placed on a given server. In a cluster setting, the workload manager

plays a crucial synergistic role in maximizing SURGE’s applicability and utility. Given sufficient workload knowledge and placement decisions, the cluster manager can indicate to each server’s OS whether I/O bandwidth resources are expected to be underutilized. The OS can then use this information to initiate I/O bandwidth salvaging, as explained in §III-B2.

By being SURGE-aware, the cluster manager can also avoid detrimental workload colocations. For example, consider workload *A* placed on a server, which is known to minimally utilize I/O resources. The cluster manager decides to colocate memory-intensive workload *B* on the same server, and notifies the server’s OS that I/O bandwidth is expected to be available for salvaging under the current workload colocation scenario. Consequently, if workload *A* completes, the cluster manager must either replace it with another workload with similar characteristics (i.e., one with similar I/O usage), or notify the OS about an impending change in available idle I/O bandwidth. The OS can then adapt by migrating workload *B*’s pages from salvage memory to the server’s primary memory.

Finally, such synergy between SURGE and the cluster manager requires the latter to be aware of the memory and I/O bandwidth demands of each deployed workload. Knowledge of workload performance characteristics is commonly required by several cluster managers, as it can greatly improve workload placement decisions, and it can be derived either via prior profiling or via explicit declaration when a workload is submitted to the cluster manager [15], [17], [26], [47].

2) Memory Traffic Split Strategy and Analytical Model:

Effective use of SURGE requires a judicious distribution of memory traffic between primary and salvage memory. We develop an analytical model, summarized in Fig. 6, to guide this decision. The model’s objective is to determine the traffic split that minimizes the overall Average Memory Access Time (AMAT) experienced by the workload. As indicated in §III-B1, our key assumption is that the cluster manager has a good estimate of memory and I/O bandwidth consumption for each workload it has deployed or is about to deploy. Given a server’s current state (i.e., deployed workloads’ memory and I/O bandwidth demands, memory system characteristics), our analytical model provides a method to derive the best theoretical traffic split between primary and salvage memory for the workload that is about to be deployed on the server.

Step ①: Load-latency profiling and AMAT modeling. The model takes as input the profiled *load-latency curves* of the server’s primary memory, salvage memory, and salvage link, derived by profiling each server configuration in the cluster *once*. These curves provide a comprehensive view of memory system behavior under varying bandwidth utilization levels. Prior work demonstrated that such representation captures the performance characteristics of real memory systems well [18].

For a workload with total memory bandwidth demand D , a fraction R of the traffic is directed to the primary memory, while the remaining $(1-R)$ is directed to the salvage memory via the salvage link, resulting in:

$$U_P = \frac{R \cdot D}{B_P}, \quad U_S = \frac{(1-R) \cdot D}{B_S} \quad (1)$$

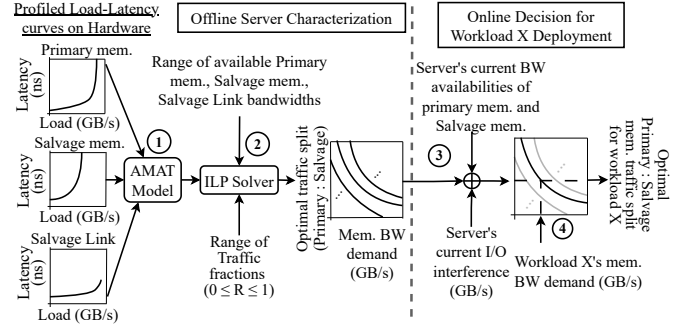


Fig. 6: Methodology to analytically determine the optimal traffic split between primary and salvage memories.

where U_P , U_S denote the utilization levels of the primary and salvage memories, respectively, and B_P , B_S denote their respective peak sustainable bandwidth.

The overall AMAT experienced by a workload for a given traffic split R is expressed as:

$$\text{AMAT}(R) = R \cdot L_P(U_P) + (1-R) \cdot [L_S(U_S) + L_{\text{ing}}(U_{\text{ing}}) + L_{\text{egr}}(U_{\text{egr}})] \quad (2)$$

where $L_P(U_P)$ and $L_S(U_S)$ represent the load-latency functions for the primary and salvage memories, while L_{ing} and L_{egr} capture the latency characteristics of the CXL interface’s ingress and egress paths, as a function of per-direction link utilization (U_{ing} and U_{egr}). U_{ing} and U_{egr} are evaluated as:

$$U_{\text{ing}} = \frac{(1-R) \cdot D \cdot \rho_{\text{rd}}}{\eta}, \quad U_{\text{egr}} = \frac{(1-R) \cdot D \cdot \rho_{\text{wr}}}{\eta} \quad (3)$$

where $\rho_{\text{rd}} = 0.75$ and $\rho_{\text{wr}} = 0.25$ correspond to a typical 3:1 read-to-write traffic ratio, and $\eta = 0.94$ denotes the effective link efficiency of the CXL interface [39]. Thus, as the fraction of traffic directed to the salvage memory increases, the ingress and egress link latencies also rise, capturing the queuing effects on the interface under higher utilization.

Step ②: Generation of optimal traffic split curves. We utilize an integer linear programming (ILP) solver to determine the traffic split between primary and salvage memory that minimizes the value of Equation (2). Thus, the ILP solver evaluates a discrete set of candidate traffic split ratios of $R \in [0.05, 1]$ in 0.05 increments, with the optimization objective

$$R^* = \arg \min_R \text{AMAT}(R) \text{ subject to } 0 \leq R \leq 1 \quad (4)$$

The solution R^* represents the theoretically *optimal traffic fraction* directed to primary memory (and, correspondingly, $1 - R^*$ to salvage memory) that minimizes aggregate AMAT for a workload with bandwidth demand D . This sequence produces one of the optimal split curves shown at the end of step ② in Fig. 6, corresponding to one system parameter combination $C = \{B_P, B_S, \text{salvage link bandwidth } (B_{\text{Lingr}} \text{ and } B_{\text{Legr}})\}$.

In a typical cluster, the existence of different system configurations implies the existence of various unique system parameter combinations C_i . Even for the same system, if a workload is already deployed, it already consumes bandwidth

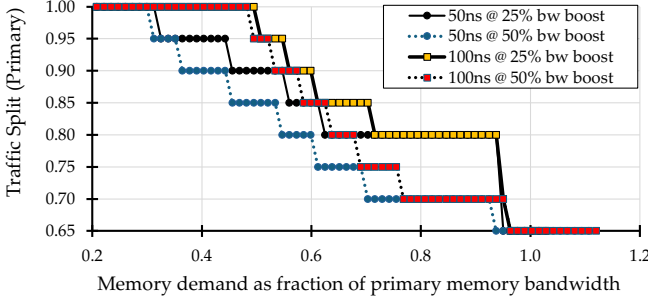


Fig. 7: Determining traffic split between primary and salvage memory as a function of memory bandwidth demand and salvage memory’s latency/bandwidth characteristics.

resources, implying that the remaining resource availability is a smaller $C' = \{B'_P, B'_S, B'_{Lingr}, B'_{Legr}\}$. Therefore, our methodology repeats step ② for a broad range of C_i values, producing a large set of traffic split curves—one for each C_i —as shown in the middle of Fig. 6. Note that this curve generation happens *offline* and only *once* for a given cluster.

Steps ③ and ④: Optimal traffic split selection at workload deployment. When the cluster scheduler deploys a new workload, it determines the optimal primary-to-salvage traffic ratio for the {workload, server} combination under consideration, in two steps. First (step ③), the server’s current bandwidth commitments (on salvage memory, primary memory, and CXL links) due to already deployed workloads dictate the target server’s resource availability C_i , corresponding to one of step ②’s generated traffic split curves. Next, in step ④, the workload’s expected memory bandwidth demand D is used to probe the selected curve, yielding the traffic split R^* to be applied for that workload under the current system state C_i . R^* is conveyed to the target server’s OS along with the workload deployment request.

Implementing the selected traffic split. The desired traffic split R^* can only be indirectly achieved via controlled data placement between primary and salvage memory. While various placement mechanisms are possible, we opt for an unintrusive page-based memory allocation approach that can be seamlessly integrated in any modern OS, as described in §IV-B.

Traffic split curve example. Fig. 7 exemplifies the use of the best traffic split curves. Each of the four curves corresponds to a salvage memory with different bandwidth and latency characteristics. We express salvage bandwidth relative to primary bandwidth, and latency as overhead over the raw DRAM access over DDR. As an example, consider a system equipped with DDR5-4800 as primary memory (38.4 GB/s nominal peak bandwidth and ~ 50 ns DRAM access latency) and salvage memory accessed over a serial link (such as CXL), which provides a bandwidth boost expressed as fraction over primary memory bandwidth. A salvage memory labeled “50 ns @ 50% boost” offers 19.2 GB/s at $(50 + 50 =) 100$ ns DRAM access latency.

The lower the memory demand, the larger the demand’s fraction that should be steered to the low-latency primary memory. As demand increases, offloading more traffic to the salvage memory reduces queuing buildup on the primary memory, reducing the overall system AMAT and improving performance. The effect of unloaded latency for a given memory bandwidth boost is significant at low demand levels, where queuing effects are negligible. At high demand levels, the system becomes bandwidth-constrained, and the contribution of queuing delays on total memory access latency starts dominating. Therefore, under high bandwidth demand, the salvage memory’s latency overhead becomes less important, as evidenced by the four curves: while higher salvage bandwidth availability results in a traffic split that steers a larger fraction away from primary memory, under high bandwidth demand, the best traffic split converges to the same value regardless of the salvage memory’s latency overhead.

IV. SURGE IMPLEMENTATION

A. Hardware Extensions

As discussed in §III-A, SURGE requires a fabric that supports dynamic multiplexing of I/O and memory traffic. Our implementation focuses on the CXL protocol, as its specification supports such dynamic multiplexing of CXL.io, .mem, and .cache traffic. While existing CXL controller IP blocks (like the one from Rambus [35]) support all three CXL protocols, they are currently designed to operate in a single mode at system initialization time. However, the CXL specification includes the “Flex Bus” feature, which supports dynamic multiplexing of traffic types and even provisions for programmable arbitration policy between them. Flex Bus provides the basic functionality required by SURGE and we are the first, to the best of our knowledge, to leverage this feature for new architectural designs that push the memory bandwidth wall.

Fig. 8 shows a block diagram of a CXL controller that performs .io and .mem traffic multiplexing using a 2-port CPU-side CXL mux [40] for traffic bifurcation between the primary I/O device and our added salvage memory device. Because in SURGE, the interface “belongs” to the I/O device, we configure the arbiter to prioritize I/O over memory traffic. At high I/O activity, such policy can penalize the—generally more latency-sensitive—memory traffic. However, prolonged high I/O activity is beyond SURGE’s target use cases.

B. Software Support

Memory traffic split via page placement. In our SURGE implementation, the OS implicitly achieves memory traffic distribution between primary and salvage memory by allocating pages in the respective memory type at the desired R^* ratio. We use a first-touch policy: every time the OS allocates a new page for a workload, it selects the primary (salvage) memory with R^* ($1 - R^*$) probability. We find that such allocation results in the intended traffic split, confirming statistical expectations.

Role of cluster manager. We assume a cluster manager aware of the fleet’s SURGE-enabled servers and at a minimum:

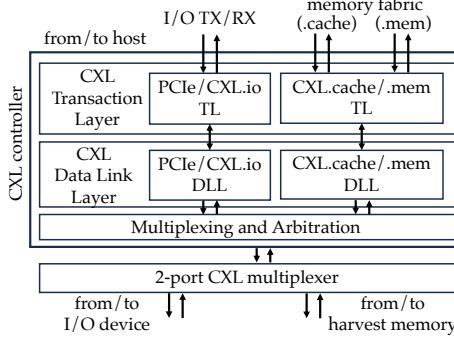


Fig. 8: I/O and memory traffic multiplexing block diagram.

- 1) Is aware of the expected average memory and I/O bandwidth use of each workload that is about to be deployed, as derived by prior workload profiling.
- 2) Given the target server’s state and workload to be deployed, determines the best traffic split R^* between primary and salvage memory as per §III-B2’s methodology, and conveys that split to the server’s OS.
- 3) Does not deploy a new I/O-intensive workload on a server where a previously deployed memory-intensive workload with permission to salvage I/O bandwidth is still active.

Advanced software support can further improve SURGE’s utility. For example, more sophisticated page placement policies than first-touch may also explicitly take the CXL salvage link’s directionality into account and place read-/write-heavy pages in salvage memory when the I/O interface has more TX/RX activity, respectively. Furthermore, dynamic memory monitoring and page migration could improve adaptability over time. For instance, advanced synergies between the cluster manager and the OS can be developed, to allow dynamic memory allocation changes during a workload’s runtime—the cluster manager could instruct the OS to free up I/O resources by scaling back on salvaging via page migration from salvage to primary memory. We focus on the demonstration of SURGE’s benefits as a novel proof-of-concept architectural technique, leaving more advanced software mechanisms to future work.

V. METHODOLOGY

Modeled system. We simulate a scaled-down version of a modern manycore server CPU. We consider two exemplary systems of such families. The AMD EPYC 9754 CPU (Bergamo) [28] features 128 cores, 12 DDR5-4800 channels, and 128 PCIe 5 lanes per socket. The Intel Xeon 6780E CPU (Sierra Forest) [20] features 144 cores, 8 DDR5-6400, and 88 PCIe 5 lanes per socket. We model a scaled down CPU with 12 cores that preserves core-to-memory-bandwidth and core-to-LLC-capacity ratios representative of such systems. We do *not* aim to derive an optimal pin allocation for the CPU (cf. §II-B) or argue for using a salvage memory *instead* of a type-3 memory over dedicated CXL links. SURGE’s novelty lies in enabling fungible use of bandwidth availability given a pre-existing, design-time CPU pin allocation between memory and

TABLE I: System parameters used for simulation in ZSim.

CPU	12 OoO cores, 2.4GHz, 4-wide, 256-entry ROB
L1	32KB L1-I&D, 8-way, 64B blocks, 4-cycle hit, inclusive
L2	512 KB, 8-way, 8-cycle hit
LLC	2MB/core, shared & inclusive, 16-way, 20-cycle hit
Memory	DDR-based (Primary): 1x DDR5-4800 channel (baseline) CXL-attached (Salvage): 50% bandwidth of primary
CXL	1x16 PCIe 5.0, 100 ns latency overhead
NIC	1x400 Gbps interface

I/O, dynamically adapting aggregate resource availability to the given workload’s bandwidth type demand.

Table I details the parameters used for cycle-level simulation in ZSim [45]. We adopt SURGE Pod as the primary instance of SURGE in most of our evaluation due to its higher utility, as discussed in §III. We assume a SURGE Pod deployment offering 50% additional memory bandwidth over a single server’s primary DDR memory bandwidth at a 100 ns latency premium (at zero load). We evaluate other bandwidth and latency values, including configurations representative of SURGE Solo deployments, as a sensitivity study (§VI-D).

Memory modeling. We model memory behavior using the Mess framework [18]. We profile the memory system of several AMD and Intel server-grade CPUs and observe similar load-latency characteristics. For our evaluation, we use the load-latency curve derived from the AMD EPYC 9754 CPU (Bergamo), as SURGE is most suitable for manycore CPUs with lower bandwidth-per-core availability. Our simulation model uses Fig. 9’s curve to determine the memory component’s latency as a function of its utilization, assessed at 1000-cycle execution intervals. We apply the same modeling method for both the primary (direct DDR) and the salvage (CXL-attached) memory.

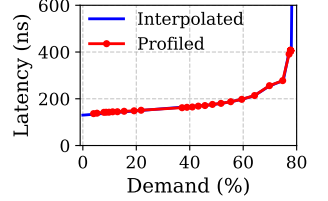


Fig. 9: Profiled DDR5-4800 memory load-to-use latency vs. demand (as % of peak) on AMD Bergamo.

CXL interface modeling. We extend ZSim’s performance models with a new CXL interface component, which models the interface’s latency, utilization, and the impact of the latter on the former. We modeled an x16 CXL link operating at 32.0 GT/s, which corresponds to a 64 GB/s raw transfer rate per direction. At the Physical and Link Layers, we assume a 68-byte flit format. Each link-layer flit consists of 64B of payload and 2B of overhead, resulting in an effective link efficiency of 0.94 after accounting for protocol and formatting overheads [39]. Beyond link-layer efficiency, we also incorporate modeling of metadata transfer overheads introduced by the transport protocol for both request and response packets exchanged between the CPU host and the CXL device, following prior work [38]. These metadata overheads reduce the effective peak bandwidth of the CXL interface. For example, for a system experiencing a 2:1 read/write ratio, the effective RX (device-to-CPU) and TX (CPU-to-device) bandwidth drops to ~80%

and $\sim 40\%$ of nominal, respectively.

Workloads. We evaluate five workloads from each of the Tailbench [22], SPEC [42], and GAP [6] benchmark suites.

- **Online services:** From Tailbench, we evaluate an open-source search engine (xapian), an in-memory key-value store (masstree), a statistical machine translation system (moses), a speech recognition engine (sphinx), and an image recognition model (imgdnn), using their default datasets. We exclude shore, silo, and specjbb as they fail to execute reliably on ZSim.
- **Throughput workloads:** From the SPEC CPU 2017 rate benchmark suite, we evaluate data compression (xz), scientific computing (bwaves, lbm, fotonik3d), and graph-based optimization (mcf) workloads in ref mode.
- **Graph analytics:** From GAP, we evaluate Breadth-First Search (bfs), Single-Source Shortest Paths (sssp), PageRank (pr), Betweenness Centrality (bc), and Triangle Counting (tc), using the Kronecker dataset.

We evaluate homogeneous scenarios, where all cores of our scaled-down CPU execute the same workload. Mixed workload scenarios yield performance approximating the average speedup achieved across single-workload experiments. We simulate 200 million instructions per core after fast-forwarding to a representative region of interest and warming up the caches. Fig. 2 shows each workload’s per-core memory bandwidth demand, derived by using an ideal memory with unconstrained bandwidth and fixed zero-load latency.

I/O traffic modeling. To evaluate I/O interference, and without loss of generality, we focus on NICs, as they are typically the highest-bandwidth I/O devices on modern servers. We emulate network traffic with a ZSim-integrated traffic generator from prior work [46] that injects and ejects packets over the simulated CXL link at configurable Poisson intervals. We also capture Data Direct I/O (DDIO) behavior: all ingress network traffic is written directly into designated ways of the last-level cache (LLC). We evaluate *high*, *medium*, and *low* NIC utilization—corresponding to 80%, 50%, and 10% of peak bandwidth—capturing a range of I/O interference scenarios.

I/O utilization scenarios. We use the combination of the aforementioned workloads and network traffic modeling to investigate a range of workload deployment scenarios encountered in cloud settings. We use a *level₁_level₂* notation to indicate the level of I/O activity on the ingress (RX) and egress (TX) path, respectively, where each level can independently take a value of the aforementioned $\{low, med, high\}$. For example, *low_low* represents a case where the CPU executes workloads with little I/O activity, while *low_high* represents a scenario with a colocated media streaming workload (e.g., Netflix [19]), featuring heavy egress (TX) path utilization.

VI. EVALUATION

We now evaluate SURGE aiming to illustrate the benefits, effectiveness, and robustness of our proposed idle I/O bandwidth salvaging technique. We address the following questions:

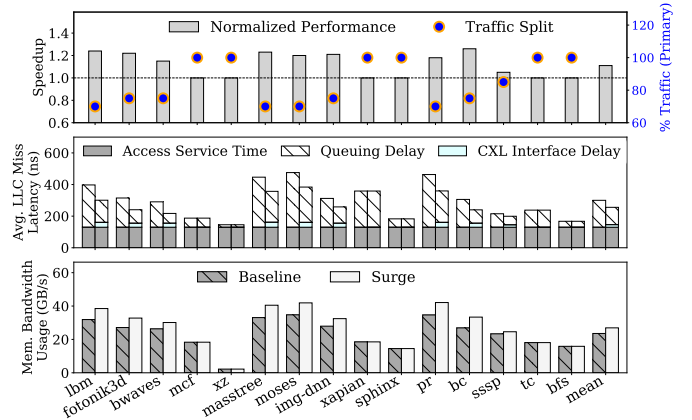


Fig. 10: Speedup, AMAT, and memory bandwidth usage for baseline vs SURGE in *low_low* networking scenario. Dots indicate the traffic split (% of traffic to primary memory) for each workload, as determined by the SURGE methodology.

- 1) What is SURGE’s performance gain headroom in a variety of workload deployment scenarios? (§VI-A, §VI-B)
- 2) How effective is our heuristic in deriving the optimal traffic split for a given workload, and how robust is SURGE’s performance to uncertainty in bandwidth utilization and I/O interference? (§VI-C)
- 3) How much do salvage link latency and bandwidth characteristics impact SURGE’s effectiveness? (§VI-D)

A. SURGE under Low I/O Utilization

Fig. 10 (top) shows the speedup achieved by SURGE over the baseline across our evaluated workloads, under the low I/O scenario. Fig. 10 (middle) presents the breakdown of average LLC miss latency (henceforth AMAT for brevity), decomposed into “Access Service Time”—i.e., the unloaded latency of retrieving data from the DRAM device—and “Queuing Delay”. In the baseline, queuing delay occurs exclusively at the primary memory, whereas in SURGE the metric represents the average queuing latency experienced across both the primary and salvage memories. “CXL Interface Delay” quantifies the time memory accesses spend on the CXL interface *on average*; for example, an access to primary memory experiences zero CXL interface delay. Finally, Fig. 10 (bottom) shows each workload’s aggregate memory bandwidth demand.

Memory-intensive workloads encountering high queuing delay due to memory bandwidth pressure in the baseline are relieved by leveraging the additional memory bandwidth afforded by the salvage memory, which is accessible over the salvage link. By splitting memory traffic between the primary and salvage memories, the system’s overall memory bandwidth increases and AMAT decreases. Across all workloads that encounter substantial queuing delay in the baseline, SURGE substantially reduces AMAT. For this subset of workloads, SURGE directs 25–30% of the traffic to the salvage memory, resulting in an average speedup of $1.2\times$ (up to $1.3\times$). It is noteworthy that while AMAT and performance are qualita-

tively correlated, the same reduction in AMAT across different workloads does not deliver the same speedup. Individual workload characteristics, such as sensitivity to memory latency, available memory-level parallelism, and temporal burstiness in memory traffic, determine the resulting speedup.

The memory bandwidth demand of several workloads (mcf, xz, xapian, sphinx, tc, bfs) is $\leq 50\%$ of the primary memory's peak theoretical availability. With such low demands, these workloads encounter minimal memory queuing in the baseline, thus SURGE's traffic split methodology directs all (or most) of the memory traffic to the primary memory. Hence, such workloads show no or marginal benefit with SURGE.

Across all workloads and with low I/O activity, SURGE achieves an average queuing delay reduction of 36%, delivering an average speedup of $1.1\times$, and up to $1.3\times$, over the baseline.

B. SURGE with Higher I/O Utilization

While the low I/O scenarios are the most intuitive use case for idle I/O bandwidth salvaging, SURGE is applicable and effective even with higher I/O activity. To highlight SURGE's breadth of applicability, we evaluate scenarios with a variety of I/O utilization levels, as outlined in §V. We use different RX_TX traffic level combinations to evaluate *low_high*, *high_low*, *med_med*, and *high_high* I/O traffic interference.

We first focus on the baseline to study each workload's behavior with increasing I/O traffic. Fig. 11a shows the results. Even though we use DDIO, increasing I/O traffic exacerbates LLC and memory bandwidth pressure, as both application and I/O data move between the LLC and the primary memory. Such network-induced traffic introduces interference in the memory hierarchy that degrades performance.

We make two observations. First, workloads exhibit different sensitivity to increasing I/O traffic interference. For example, xz, which has the lowest bandwidth requirements, remains virtually unaffected, xapian, sssp, and tc exhibit sharp performance drops as I/O utilization increases, and the remaining workloads experience different degrees of more gradual degradation. Second, workloads are affected differently by RX and TX interference, with tc and sssp more sensitive to the former, and others (like mcf, masstree, pr) more sensitive to the latter. Across workloads, a medium or high interference on both RX and TX is detrimental to performance.

Fig. 11b shows the impact of I/O utilization on SURGE's effectiveness. The *low_low* configuration represents the scenario studied in §VI-A, *low_high* represents TX-heavy scenarios, such as media streaming, while *high_low* represents RX-heavy scenarios. SURGE yields a stable speedup over the baseline, across all I/O utilization levels, of $\sim 1.1\times$ on average. The results indicate that SURGE effectively adjusts the traffic split between primary and salvage memory, balancing bandwidth pressure on primary memory with I/O interface and salvage memory bandwidth availability to minimize the contribution of queuing delays on AMAT.

As I/O activity increases, SURGE's methodology reevaluates the optimal traffic split between primary and salvage memory. Higher I/O activity means less available bandwidth to salvage

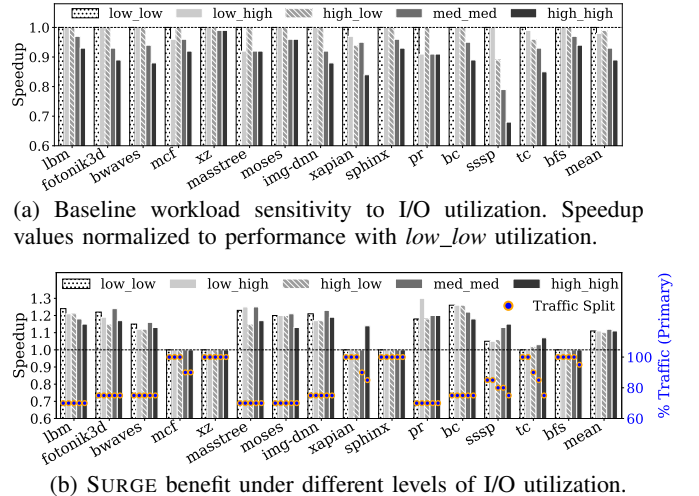


Fig. 11: Impact of I/O traffic interference. $level_1_level_2$ on the legends indicates RX_TX path utilization.

on the I/O link, but also increased bandwidth pressure on the primary memory due to network induced memory traffic, pushing queuing delays higher. With few exceptions, the SURGE-determined optimal traffic split remains stable across I/O utilization level. This is because (i) even under higher I/O utilization, the I/O interface offers considerable bandwidth availability to complement the primary memory's bandwidth, and (ii) the increase in the I/O interface's contributed queuing delay at higher utilization is smaller than the primary memory's high queuing delays under high memory bandwidth demand. Even in the few cases where higher I/O interference shifts the traffic split (mcf, xapian, sssp, tc, bfs), SURGE places *less* traffic to primary memory, indicating that queuing at the primary memory bandwidth is more detrimental than queuing on the I/O interface, thereby determining that shifting more traffic to the latter is overall beneficial. As a result, even with *high_high* I/O activity, SURGE yields speedups of up to $1.2\times$. Importantly, even when SURGE does not benefit a workload, it has a performance-neutral effect, delivering performance on par with the baseline.

Finally, in a few workload cases, like xapian, sssp, and tc, SURGE delivers a higher speedup under higher I/O utilization. The increased speedup is because the baseline's performance degrades fast, while SURGE offers better performance robustness, as its enforced traffic split manages to absorb the detrimental bandwidth interference experienced by the baseline at the primary memory.

C. Robustness of the SURGE Traffic Split Methodology

SURGE's traffic split methodology relies on workload knowledge, specifically their memory bandwidth demand and I/O activity levels, derived from profiling. In this section, we study our traffic split approach's robustness to imprecision in such knowledge, due to inaccurate profiling or fluctuations in memory bandwidth utilization and I/O interference.

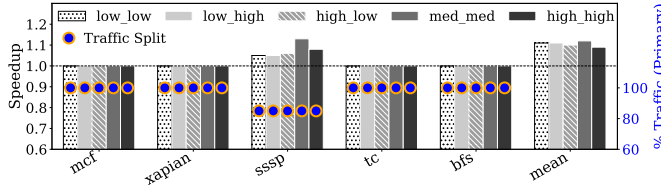


Fig. 12: Robustness to I/O interference. Traffic split configured expecting *low_low* I/O traffic in all cases. The plot shows only the subset of workloads that are sensitive to the SURGE-selected traffic split, while the mean refers to all 15 workloads.

1) Performance sensitivity to unexpected I/O interference:

We first focus on the impact of I/O interference uncertainty; namely, when I/O utilization ends up being higher than expected at the time of a workload’s deployment—for example, expecting *low* utilization but encountering *medium* or *high* instead, which represents a substantial spike of $5 \times 8 \times$, respectively. Fig. 11b already showed that the optimal traffic split for a given workload is largely insensitive to the I/O utilization level. In other words, for most workloads, the SURGE traffic split methodology would determine the same traffic split value across all the I/O utilization levels we consider.

Fig. 12 focuses on SURGE’s performance for the five workloads that benefit from adjusting the traffic split according to the I/O activity level. Performance for the remaining ten workloads is not shown, because it matches Fig. 11b’s results. Of those five workloads, *sssp* still preserves some performance gains with SURGE. While the remaining four lose any performance gains when I/O utilization is higher than the expected *low_low*, *none* of them experiences a slowdown, performing on par with the baseline. For some cases, like *mcf* and *xapian* under *med_med* and *mcf* under *high_high*, a comparison between Fig. 11b and Fig. 12 reveals that SURGE performs on par with the baseline, despite a difference in the traffic split used in the two experiments. This behavior is attributed to our observation that the optimal traffic split is a *range* rather than a single point, as explained next in §VI-C2 and Fig. 13.

Overall, SURGE delivers robust performance results even under unexpected I/O traffic interference (whether sustained or instantaneous in the form of temporal spikes). No workload experiences a slowdown, average speedup remains substantial at $\sim 1.1 \times$ across I/O interference levels, with some workloads still experiencing a performance gain of up to $1.25 \times$.

2) Performance sensitivity to traffic split:

For our next robustness analysis, we use the workloads *without any I/O interference* to exclusively focus on memory bandwidth utilization uncertainty. Fig. 13 shows the resulting AMAT and speedup as a function of the applied traffic split. In the interest of space, we only indicatively show data for the *bc* workload; similar trends hold for all workloads. Evidently, the selected traffic split critically affects performance: the best choice can yield a speedup of $1.2 \times$, but a poor choice can incur a 67% slowdown. For *bc*, the optimal primary:salvage split in

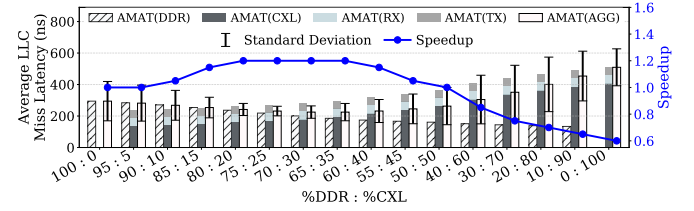


Fig. 13: AMAT and speedup for the *bc* workload across the range of possible primary:salvage memory traffic splits. Whiskers show standard deviation.

a deployment scenario without I/O interference falls in the 80:20 to 65:35 range. However, there is a wide traffic split range from 85:15 to 60:40 where SURGE yields substantial performance gains of $1.15 \times$ or higher. Given the breadth of this range, SURGE is robust to uncertainty or fluctuations in memory bandwidth usage.

SURGE’s performance gains primarily stem from reducing the memory system’s AMAT. Fig. 13 confirms that the highest speedup is achieved by the configuration with the lowest AMAT. The whiskers on Fig. 13’s aggregate AMAT bars highlight an additional significant benefit of SURGE. In addition to reducing AMAT, SURGE also reduces memory access latency variance, because queuing delay—which significantly fluctuates over time due to temporal bursts in memory bandwidth demand—becomes a smaller contributor to overall latency. Higher memory access time predictability additionally contributes to performance improvement, as observed in prior work [13].

SURGE’s methodology determines a traffic split based on average bandwidth utilization derived from profiling. We now evaluate how close the derived traffic split is to the optimal (i.e., best-performing split). We derive the latter experimentally, using a primary:salvage split sweep in 5% increments.

Fig. 14 (top) shows that, across all workloads, the SURGE methodology’s theoretically derived traffic split matches or is very close to the practically optimal. Importantly, there is a significant margin of deviation from the optimal split within which SURGE performs close to its maximum potential: the error bars indicate the traffic split range that still delivers performance within 10% of the optimal split. The reason for such robustness is that there is a wide plateau around the performance peak, as previously demonstrated in Fig. 13.

Fig. 14 (bottom) shows each workload’s memory demand, and the speedup achieved with the SURGE-derived and optimal split, respectively. Indeed, SURGE’s achieved speedup is very close to the one achieved with an optimal split: within 1% on average and at most within 5%.

D. Sensitivity to Salvage Link Latency and Bandwidth

We conclude our evaluation with a sensitivity study on the latency and bandwidth characteristics of the CXL-attached salvage memory. We express salvage memory bandwidth in terms relative to the primary memory’s bandwidth. Fig. 15 shows SURGE’s attainable speedup for 16 bandwidth-latency

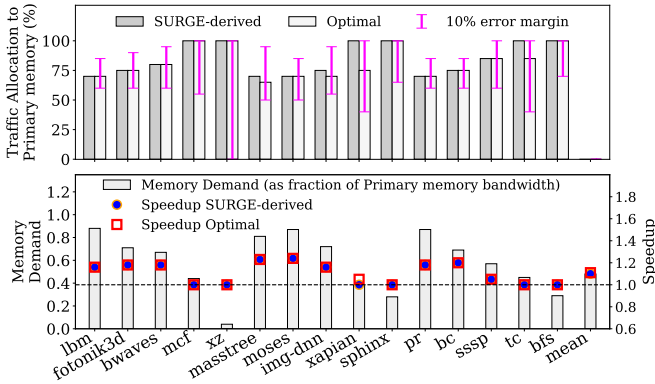


Fig. 14: Deviation of SURGE-derived traffic split from optimal split, and impact on performance in *no I/O* scenarios.

combinations and six of our workloads with *low_low* I/O utilization. 50% bandwidth boost at 100 ns latency premium is the configuration used throughout the evaluation, which we consider a reasonable design point for a SURGE Pod deployment. Configurations with lower bandwidth boost and potentially lower latency (e.g., 25% boost, 50 ns) are more likely for SURGE Solo deployments, as discussed in §III-A3.

While the sensitivity of workloads to the salvage memory's bandwidth-latency characteristics differs, the same key observation holds across the board: for the bandwidth-strapped scenarios SURGE targets, bandwidth is more important than unloaded latency penalty. The reason is that SURGE is a technique that shines under bandwidth scarcity, where the primary memory experiences latency spikes due to queuing. In such cases, even a 200 ns unloaded latency premium is preferable, if the memory system can be brought to an operational point prior to the region of exponential queuing delays. Workloads with lower bandwidth demands that don't benefit from SURGE, like *mcf* (not shown), are insensitive to salvage memory latency premium, because the SURGE traffic split methodology diverts less (or no) traffic to the salvage memory. The effect of latency is more pronounced at higher bandwidth availability, where the contribution of queuing to AMAT is less pronounced. Our sensitivity study highlights that the higher bandwidth that SURGE Pod is likely to be able to afford can more than offset its higher latency premium.

VII. RELATED WORK

High-end processors feature increasing core counts for throughput gains, with the aim of improving resource consolidation and TCO. However, commensurately scaling memory bandwidth availability using DDR technology alone is challenging, resulting in reducing the memory bandwidth availability per core. Hence, such manycore processors cannot be effectively utilized when handling memory-intensive workloads. Some recent high-end CPUs alleviate the memory bandwidth wall by deploying HBM [23], [32] or large die-stacked SRAM [1]. However, in addition to their high cost, such exotic solutions suffer from severely limited capacity [34].

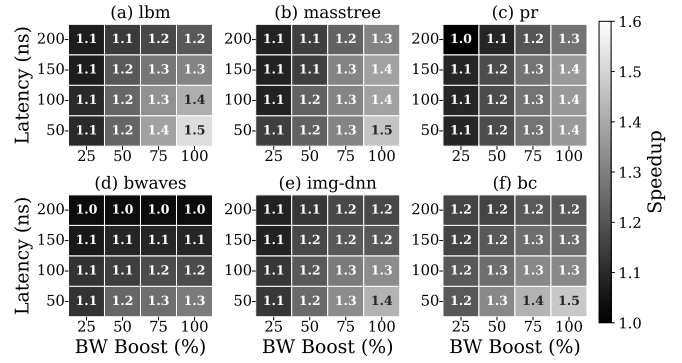


Fig. 15: Impact of salvage memory's bandwidth-latency characteristics on SURGE's effectiveness. SURGE Solo/Pod deployments are more likely to offer characteristics landing toward the bottom left/top right corner, respectively.

Memory tiering. In the context of CXL, recent works have explored using CXL-attached memory as a secondary tier to expand both capacity and bandwidth [4], [21], [27], [48]. However, CXL-based tiering requires careful hardware-software co-design to mitigate the high serial link latency [3], [41]. As in SURGE, careful page placement across the memory tiers plays an important role in maximizing performance.

Memory bandwidth boosting. BATMAN [14] proposes spreading a workload's dataset across planar and die-stacked DRAM to maximize aggregate memory bandwidth availability. Caption [44] aims to improve the performance of bandwidth-intensive applications by leveraging CXL memory devices for bandwidth expansion, and uses a linear Machine Learning model to perform bandwidth-aware page allocation across the memory tiers. Sehgal et al. [37] propose software-based weighted interleaving of pages to leverage the bandwidth of DDR and CXL memory, considering the workload characteristics and performance characteristics of memories to various memory read/write patterns. Coaxial proposes complete replacement of the prevalent DDR-based memory system with a bandwidth-rich CXL-based memory system [12], but such radical approach can hurt performance under low system utilization. In contrast to all prior work deploying and managing a secondary memory tier to boost bandwidth, SURGE multiplexes existing (primarily I/O) interfaces to opportunistically boost memory bandwidth availability. SURGE is the first extensive study of the opportunities arising from the CXL-enabled fungibility of I/O and memory traffic, and the first system to leverage that capability to dynamically salvage idle I/O bandwidth, convert it to additional memory bandwidth for memory-bound workload acceleration.

Page placement. SURGE leverages controlled page placement as a way to split traffic between the tiered primary-salvage memory system. We found weighted first-touch page placement sufficient for the simple proof-of-concept deployment scenarios we evaluated. However, more complex cases with workload churn would require periodic re-evaluation of each

workload's traffic split and support for more sophisticated page placement and migration techniques. There are several such mechanisms in the literature, both software-based [2], [25], [27], [33], [36], [50] and hardware-assisted [11], [31].

VIII. CONCLUSION

Modern manycore CPUs encounter increasing memory bandwidth pressure, as off-chip bandwidth scales slower than core counts. This paper identifies an opportunity to ameliorate this pressure by introducing SURGE, a technique that dynamically salvages idle I/O bandwidth and converts it to a memory bandwidth boost. SURGE realizes such bandwidth salvaging by leveraging the modern CXL interface's capability for dynamic multiplexing of I/O and memory traffic. We introduce a design that combines SURGE's architectural capability with software support that determines the best traffic split between primary and salvage memory, with the goal of minimizing each workload's AMAT. Our evaluation shows that SURGE delivers performance gains of up to $1.3\times$ when the I/O subsystem is largely underutilized, and up to $1.2\times$ under substantial I/O activity. SURGE represents a novel, effective, and timely technique to boost memory bandwidth availability for modern bandwidth-strapped manycore processors.

ACKNOWLEDGMENTS

We thank Marina Vemmou for extensive help with ZSim, particularly with the integration of NIC traffic and DDIO behavior; Hamed Seyedroudbari for insightful discussions; Albert Cho and Prachatos Mitra for feedback that improved the paper; and Balaadithya Uppalapati for discussions that helped firm up the ILP solver component of SURGE's traffic split methodology. This work was supported by the National Science Foundation, award SHF-2333049.

REFERENCES

- [1] Advanced Micro Devices, Inc., "Nothing Stacks Up to Epyc: Elevating Data Center Computing with AMD 3D V-Cache," 2021, <https://www.amd.com/content/dam/amd/en/documents/epyc-business-docs/product-briefs/3d-vcache.pdf>.
- [2] N. Agarwal and T. F. Wenisch, "Thermostat: Application-transparent page management for two-tiered main memory," in *Proceedings of the Twenty-Second International Conference on Architectural Support for Programming Languages and Operating Systems, ASPLOS 2017, Xi'an, China, April 8-12, 2017*, Y. Chen, O. Temam, and J. Carter, Eds. ACM, 2017, pp. 631–644. [Online]. Available: <https://doi.org/10.1145/3037697.3037706>
- [3] M. K. Aguilera, E. Amaro, N. Amit, E. Hunhoff, A. Yelam, and G. Zellweger, "Memory disaggregation: why now and what are the challenges," *ACM SIGOPS Oper. Syst. Rev.*, vol. 57, no. 1, pp. 38–46, 2023. [Online]. Available: <https://doi.org/10.1145/3606557.3606563>
- [4] M. Arif, K. Assogba, M. M. Rafique, and S. Vazhkudai, "Exploiting cxl-based memory for distributed deep learning," in *Proceedings of the 51st International Conference on Parallel Processing, ICPP 2022, Bordeaux, France, 29 August 2022 - 1 September 2022*. ACM, 2022, pp. 19:1–19:11. [Online]. Available: <https://doi.org/10.1145/3545008.3545054>
- [5] Backblaze, "The SSD Edition: 2023 Drive Stats Mid-Year Review," 2023, <https://www.backblaze.com/blog/ssd-edition-2023-mid-year-drive-stats-review/>.
- [6] S. Beamer, K. Asanovic, and D. A. Patterson, "The GAP benchmark suite," *CoRR*, vol. abs/1508.03619, 2015. [Online]. Available: <http://arxiv.org/abs/1508.03619>
- [7] T. Benson, A. Akella, and D. A. Maltz, "Network traffic characteristics of data centers in the wild," in *Proceedings of the 10th ACM SIGCOMM Workshop on Internet Measurement (IMC)*, 2010, pp. 267–280.
- [8] T. Benson, A. Anand, A. Akella, and M. Zhang, "Understanding data center traffic characteristics," in *Proceedings of the 1st ACM SIGCOMM 2009 Workshop on Research on Enterprise Networking (WREN)*, 2009, pp. 65–72.
- [9] D. S. Berger, Y. Zhong, P. Zardoshti, S. Teng, F. Kazhamiaka, and R. Fonseca, "Octopus: Scalable Low-Cost CXL Memory Pooling," *CoRR*, vol. abs/2501.09020, 2025.
- [10] A. Chatterjee, P. Ellerjee, V. J. M. III, J.-C. Park, K. won Choi, and K. Puttaswamy, "System Level Power-Performance Trade-Offs in Embedded Systems Using Voltage and Frequency Scaling of Off-Chip Buses and Memory," in *Proceedings of the 15th International Symposium on System Synthesis*, 2002, pp. 225–230.
- [11] A. Cho and A. Daglis, "StarNUMA: Mitigating NUMA Challenges with Memory Pooling," in *Proceedings of the 57th Annual IEEE/ACM International Symposium on Microarchitecture (MICRO)*, 2024, pp. 997–1012.
- [12] A. Cho, A. Saxena, M. Qureshi, and A. Daglis, "COAXIAL: A CXL-Centric Memory System for Scalable Servers," in *Proceedings of the 2024 ACM/IEEE Conference on Supercomputing (SC)*, 2024, p. 95.
- [13] A. Cho, A. Saxena, M. K. Qureshi, and A. Daglis, "A case for cxl-centric server processors," *CoRR*, vol. abs/2305.05033, 2023.
- [14] C.-C. Chou, A. Jaleel, and M. K. Qureshi, "BATMAN: techniques for maximizing system bandwidth of memory systems with stacked-DRAM," in *Proceedings of the 2017 International Symposium on Memory Systems (MEMSYS)*, 2017, pp. 268–280.
- [15] Christina Delimitrou and Christos Kozyrakis, "Quasar: resource-efficient and QoS-aware cluster management," in *Proceedings of the 19th International Conference on Architectural Support for Programming Languages and Operating Systems (ASPLOS-XIX)*, 2014, pp. 127–144.
- [16] CXL Consortium, "Compute Express Link (CXL) Specification, Revision 3.2, Version 1.0," 2024. [Online]. Available: https://computeexpresslink.org/wp-content/uploads/2024/11/CXL-Specification_rev3p2_ver1p0_2024October2_evalcopy.pdf
- [17] C. Delimitrou and C. Kozyrakis, "Paragon: QoS-aware scheduling for heterogeneous datacenters," in *Proceedings of the 18th International Conference on Architectural Support for Programming Languages and Operating Systems (ASPLOS-XVIII)*, 2013, pp. 77–88.
- [18] P. Esmaili-Dokht, F. Sgherzi, V. S. Girelli, I. Boixaderas, M. Carmin, A. Monemi, A. Armejach, E. Mercadal, G. Llort, P. Radokovic, M. Moretó, J. Giménez, X. Martorell, E. Ayguadé, J. Labarta, E. Conflanieri, R. Dubey, and J. Adlard, "A Mess of Memory System Benchmarking, Simulation and Application Profiling," in *Proceedings of the 57th Annual IEEE/ACM International Symposium on Microarchitecture (MICRO)*, 2024, pp. 136–152.
- [19] D. Gallatin, "The ‘other’ FreeBSD optimizations used by Netflix to serve video at 800Gb/s from a single server," *EuroBSDCon*, 2022.
- [20] Hassan Mujtaba, "Intel Granite Rapids & Sierra Forest Xeon CPU Detailed In Avenue City Platform Leak: Up To 500W TDP & 12-Channel DDR5," 2023. [Online]. Available: <https://wccftech.com/intel-granite-rapids-sierra-forest-xeon-cpu-detailed-in-avenue-city-platform-leak-up-to-500w-tdp-12-channel-ddr5/>
- [21] W. Huang, M. Sha, M. Lu, Y. Chen, B. He, and K. Tan, "Bandwidth expansion via CXL: A pathway to accelerating in-memory analytical processing," in *Proceedings of Workshops at the 50th International Conference on Very Large Data Bases, VLDB 2024, Guangzhou, China, August 26–30, 2024*. VLDB.org, 2024. [Online]. Available: https://vldb.org/workshops/2024/proceedings/ADMS/ADMS24_01.pdf
- [22] H. Kasture and D. Sánchez, "Tailbench: a benchmark suite and evaluation methodology for latency-critical applications," in *Proceedings of the 2016 IEEE International Symposium on Workload Characterization (IISWC)*, 2016, pp. 3–12.
- [23] J. Kim and Y. Kim, "HBM: Memory solution for bandwidth-hungry processors," in *Hot Chips Symposium*, 2014, pp. 1–24.
- [24] H. Li, D. S. Berger, L. Hsu, D. Ernst, P. Zardoshti, S. Novakovic, M. Shah, S. Rajadnya, S. Lee, I. Agarwal, M. D. Hill, M. Fontoura, and R. Bianchini, "Pond: CXL-Based Memory Pooling Systems for Cloud Platforms," in *ASPLOS (2)*, 2023, pp. 574–587.
- [25] J. Liu, H. Hadian, H. Xu, and H. Li, "Tiered memory management beyond hotness," in *19th USENIX Symposium on Operating Systems Design and Implementation, OSDI 2025, Boston, MA, USA, July 7-9, 2025*, L. Zhou and Y. Zhou, Eds. USENIX Association, 2025, pp. 731–747. [Online]. Available: <https://www.usenix.org/conference/osdi25/presentation/liu>

[26] D. Lo, L. Cheng, R. Govindaraju, P. Ranganathan, and C. Kozyrakis, “Heracles: improving resource efficiency at scale,” in *Proceedings of the 42nd International Symposium on Computer Architecture (ISCA)*, 2015, pp. 450–462.

[27] H. A. Maruf, H. Wang, A. Dhanotia, J. Weiner, N. Agarwal, P. Bhattacharya, C. Petersen, M. Chowdhury, S. O. Kanaujia, and P. Chauhan, “TPP: Transparent Page Placement for CXL-Enabled Tiered Memory,” *Proceedings of the 28th International Conference on Architectural Support for Programming Languages and Operating Systems (ASPLOS XXVIII)*, 2023.

[28] H. Mujtaba, “AMD EPYC Bergamo ‘Zen 4C’ CPUs Being Deployed In 1H 2023 To Tackle Arm CPUs, Instinct MI300 APU Back In Labs,” 2022. [Online]. Available: <https://wccftech.com/amd-epyc-bergamo-zен-4c-cpus-being-deployed-in-1h-2023-tackle-arm-instinct-mi300-apu-back-in-labs/amp/>

[29] D. Narayanan, E. Thereska, A. Donnelly, S. Elnikety, and A. I. T. Rowstron, “Migrating server storage to SSDs: analysis of tradeoffs,” in *Proceedings of the 2009 EuroSys Conference*, 2009, pp. 145–158.

[30] B. Nitin, W. Randy, I. Shinichiro, F. Eiji, R. Shibata, S. Yumiko, and O. Megumi, “DDR5 design challenges,” in *2018 IEEE 22nd Workshop on Signal and Power Integrity (SPI)*, 2018, pp. 1–4.

[31] V. Petrucci, F. Zacarias, and D. Roberts, “A limits study of memory-side tiering telemetry,” *CoRR*, vol. arXiv:2508.09351, 2025. [Online]. Available: <https://www.arxiv.org/abs/2508.09351>

[32] U. Pirzada, “Intel Announces The Worlds First x86 CPU With HBM Memory: Xeon Max ‘Sapphire Rapids’ Data Center CPU,” 2022, <https://wccftech.com/intel-announces-the-worlds-first-x86-cpu-with-hbm-memory-xeon-max-sapphire-rapids-data-center-cpu/>.

[33] J. Póvoas, J. Barreto, B. Chominski, A. Gonçalves, F. Karabeinikau, M. Maciejewski, J. Schmiegel, and K. Storozhuk, “Better memory tiering, right from the first placement,” in *Proceedings of the 16th ACM/SPEC International Conference on Performance Engineering, ICPE 2025, Toronto, ON, Canada, May 5-9, 2025*, M. Litoiu, E. Smirni, A. V. Papadopoulos, and K. Wolter, Eds. ACM, 2025, pp. 253–265. [Online]. Available: <https://doi.org/10.1145/3676151.3719378>

[34] M. K. Qureshi and G. H. Loh, “Fundamental Latency Trade-off in Architecting DRAM Caches: Outperforming Impractical SRAM-Tags with a Simple and Practical Design,” in *Proceedings of the 45th Annual IEEE/ACM International Symposium on Microarchitecture (MICRO)*, 2012, pp. 235–246.

[35] Rambus, “Compute Express Link (CXL) Controller IP,” 2024, <https://www.rambus.com/interface-ip/cxl/>.

[36] A. Raybuck, T. Stamler, W. Zhang, M. Erez, and S. Peter, “Hemem: Scalable tiered memory management for big data applications and real NVM,” in *SOSP ’21: ACM SIGOPS 28th Symposium on Operating Systems Principles, Virtual Event / Koblenz, Germany, October 26-29, 2021*, R. van Renesse and N. Zeldovich, Eds. ACM, 2021, pp. 392–407. [Online]. Available: <https://doi.org/10.1145/3477132.3483550>

[37] R. Sehgal, V. Tanna, V. Petrucci, and A. Godbole, “Optimizing system memory bandwidth with micron CXL memory expansion modules on intel xeon 6 processors,” *CoRR*, vol. abs/2412.12491, 2024. [Online]. Available: <https://doi.org/10.48550/arXiv.2412.12491>

[38] D. D. Sharma, “Compute Express Link®: An open industry-standard interconnect enabling heterogeneous data-centric computing,” in *Proceedings of the 2022 Annual Symposium on High-Performance Interconnects*, 2022, pp. 5–12.

[39] D. D. Sharma, R. Blankenship, and D. S. Berger, “An introduction to the compute express link (CXL) interconnect,” *ACM Comput. Surv.*, vol. 56, no. 11, pp. 290:1–290:37, 2024. [Online]. Available: <https://doi.org/10.1145/3669900>

[40] V. Sheth, “The CXL Arbitrator & Multiplexer in a Nutshell.” [Online]. Available: <https://any silicon.com/the-cxl-arbitrator-multiplexer-in-a-nutshell/>

[41] J. Sim, S. Ahn, T. Ahn, S. Lee, M. Rhee, J. Kim, K. Shin, D. Moon, E. Kim, and K. Park, “Computational cxl-memory solution for accelerating memory-intensive applications,” in *IEEE International Symposium on High-Performance Computer Architecture, HPCA 2024, Edinburgh, United Kingdom, March 2-6, 2024*. IEEE, 2024, p. 615. [Online]. Available: <https://doi.org/10.1109/HPCA57654.2024.00053>

[42] Standard Performance Evaluation Corporation, “SPEC CPU2017 Benchmark Suite.” [Online]. Available: <http://www.spec.org/cpu2017/>

[43] P. Stanley-Marbell, V. C. Cabezas, and R. P. Luijten, “Pinned to the walls: impact of packaging and application properties on the memory and power walls,” in *Proceedings of the 2011 International Symposium on Low Power Electronics and Design*, 2011, pp. 51–56.

[44] Y. Sun, Y. Yuan, Z. Yu, R. Kuper, C. Song, J. Huang, H. Ji, S. Agarwal, J. Lou, I. Jeong, R. Wang, J. H. Ahn, T. Xu, and N. S. Kim, “Demystifying CXL memory with genuine cxl-ready systems and devices,” in *Proceedings of the 56th Annual IEEE/ACM International Symposium on Microarchitecture, MICRO 2023, Toronto, ON, Canada, 28 October 2023 - 1 November 2023*. ACM, 2023, pp. 105–121. [Online]. Available: <https://doi.org/10.1145/3613424.3614256>

[45] D. Sánchez and C. Kozyrakis, “ZSim: fast and accurate microarchitectural simulation of thousand-core systems,” in *Proceedings of the 40th International Symposium on Computer Architecture (ISCA)*, 2013, pp. 475–486.

[46] M. Vemmou, A. Cho, and A. Daglis, “Patching up Network Data Leaks with Sweeper,” in *Proceedings of the 55th Annual IEEE/ACM International Symposium on Microarchitecture (MICRO)*, 2022, pp. 464–479.

[47] A. Verma, L. Pedrosa, M. Korupolu, D. Oppenheimer, E. Tune, and J. Wilkes, “Large-scale cluster management at Google with Borg,” in *Proceedings of the 2015 EuroSys Conference*, 2015, pp. 18:1–18:17.

[48] M. Vuppala and R. Agarwal, “Tiered Memory Management: Access Latency is the Key!” in *Proceedings of the 30th ACM Symposium on Operating Systems Principles (SOSP)*, 2024, pp. 79–94.

[49] W. A. Wulf and S. A. McKee, “Hitting the memory wall: implications of the obvious,” *SIGARCH Comput. Archit. News*, vol. 23, no. 1, pp. 20–24, 1995.

[50] L. Xiang, Z. Lin, W. Deng, H. Lu, J. Rao, Y. Yuan, and R. Wang, “Nomad: Non-exclusive memory tiering via transactional page migration,” in *18th USENIX Symposium on Operating Systems Design and Implementation, OSDI 2024, Santa Clara, CA, USA, July 10-12, 2024*, A. Gavrilovska and D. B. Terry, Eds. USENIX Association, 2024, pp. 19–35. [Online]. Available: <https://www.usenix.org/conference/osdi24/presentation/xiang>

[51] X. Zhang, K. Liu, Y. Hui, X. Zheng, Y. Chang, Y. Shan, G. Zhang, K. Zhang, Y. Bao, M. Chen, and C. Wang, “DRack: A CXL-Disaggregated Rack Architecture to Boost Inter-Rack Communication,” in *USENIX ATC*, 2025, pp. 1261–1279.

[52] Q. Zhu, S. Venkataraman, C. Ye, and A. Chandrasekhar, “Package design challenges and optimizations in density efficient (Intel® Xeon® processor D) SoC,” in *2016 IEEE Electrical Design of Advanced Packaging and Systems (EDAPS)*, 2016.